The Lifetime of Nitrogen Oxides in an Isoprene Dominated Forest

Paul S. Romer[1], Kaitlin C. Duffey[1], Paul J. Wooldridge[1], Hannah M. Allen[2,3], Benjamin R. Ayres[2], Steven S. Brown[4], William H. Brune[5], John D. Crounse[6], Joost de Gouw[4,7], Danielle C. Draper[2,8], Philip A. Feiner[5], Juliane L. Fry[2], Allen H. Goldstein[9,10], Abigail Koss[4,7], Pawel K. Misztal[10], Tran B. Nguyen[6,11], Kevin Olson[9], Alex P. Teng[6], Paul O. Wennberg[6,12], Robert J. Wild[4,7], Li Zhang[5], and Ronald C. Cohen[1,13]

[1]Department of Chemistry, University of California at Berkeley, Berkeley, CA, USA

[2]Department of Chemistry, Reed College, Portland, OR, USA

[3]Division of Chemistry and Chemical Engineering, California Institute of Technology, Pasadena, CA, USA

[4]Chemical Sciences Division, Earth System Research Laboratory, National Oceanic and Atmospheric Administration, Boulder, CO, USA

[5]Department of Meteorology, Pennsylvania State University, University Park, PA, USA.

[6]Division of Geological and Planetary Sciences, California Institute of Technology, Pasadena, CA, USA

[7]Cooperative Institute for Research in Environmental Sciences, University of Colorado, Boulder, CO, USA

[8]Department of Chemistry, University of California, Irvine, CA, USA

[9]Department of Civil and Environmental Engineering, University of California at Berkeley, Berkeley, CA, USA

[10]Department of Environmental Science, Policy and Management, University of California at Berkeley, Berkeley, CA, USA

[11]Department of Environmental Toxicology, University of California, Davis, CA, USA

[12]Division of Engineering and Applied Science, California Institute of Technology, Pasadena, CA, USA

[13]Department of Earth and Planetary Sciences, University of California at Berkeley, Berkeley, CA, USA

Correspondence to: Ronald C. Cohen (rccohen@berkeley.edu)

Abstract. The lifetime of nitrogen oxides (NO_x) affects the concentration and distribution of NO_x and the spatial patterns of nitrogen deposition. Despite its importance, the lifetime of NO_x is poorly constrained in rural and remote continental regions. We use measurements from a site in central Alabama during the Southern Oxidant and Aerosol Study (SOAS) in summer 2013 to provide new insights into the chemistry of NO_x and NO_x reservoirs. We find that the lifetime of NO_x during the daytime is controlled primarily by the production and loss of alkyl and multifunctional nitrates (ΣANs). During SOAS, ΣAN production was rapid, averaging 90 ppt hr^{-1} during the day, and occurred predominantly during isoprene oxidation. Analysis of the ΣAN and HNO_3 budgets indicate that ΣANs have an average lifetime of under 2 hours, and that approximately 45% of the ΣANs produced at this site are rapidly hydrolyzed to produce nitric acid. We find that ΣAN hydrolysis is the largest source of HNO_3 and the primary pathway to permanent removal of NO_x from the boundary layer in this location. Using these new constraints on the fate of ΣANs, we find that the NO_x lifetime is 11 ± 5 hours under typical midday conditions. The lifetime is extended by storage of NO_x in temporary reservoirs, including acyl peroxy nitrates and ΣANs.

1 Introduction

The concentration and chemistry of nitrogen oxides (NO_x) in Earth's troposphere has a significant and non-linear effect on the oxidative capacity of the atmosphere. This in turn affects the production, composition, and aging of aerosols and the lifetime of greenhouse gases such as methane. Concentrations of NO_x control the production of ozone, a respiratory health hazard, important oxidant, and greenhouse gas. In addition, the deposition of reactive nitrogen is an important source of nutrients in some ecosystems (e.g. Fowler et al., 2013).

NO_x is emitted by both anthropogenic and biogenic sources, including motor vehicles, power plants, forest fires, and soil bacteria (e.g. Dallmann and Harley, 2010; Mebust and Cohen, 2014; Hudman et al., 2012), and is temporarily or permanently removed from the atmosphere by chemical conversion to higher oxides of nitrogen. Across much of the globe, the balance of these sources and sinks is in a period of dramatic change, with large reductions of NO_x emissions occurring in North America and Europe and significant increases occurring in Asia (e.g. Russell et al., 2012; Curier et al., 2014; Reuter et al., 2014). Understanding the effects of changes in NO_x emissions on the concentration and spatial distribution of NO_x requires detailed knowledge of the chemistry and transport of NO_x and NO_x reservoirs. These reservoirs are poorly understood and represent a significant uncertainty in analyses of NO_x emissions and ozone production (e.g. Ito et al., 2007; Browne and Cohen, 2012; Mao et al., 2013).

The net chemical loss of NO_x is difficult to directly observe. Observational methods for determining the lifetime of NO_x are easiest to apply in the outflow of isolated emissions, where the declining concentration of NO_x or the changing ratio of NO_x to total reactive nitrogen (NO_y) provide clear evidence for NO_x loss (e.g. Ryerson et al., 1998; Dillon et al., 2003; Alvarado et al., 2010; Valin et al., 2013). In rural and remote regions, emissions and concentrations of NO_x and NO_y are typically slowly varying over large distances (e.g. Browne et al., 2013), preventing the loss of NO_x from being directly observable. Nor can the lifetimes found in plume studies be easily translated into an appropriate lifetime in the regional background. Short-lived NO_x reservoirs such as Peroxy Acyl Nitrate (PAN) can efficiently remove NO_x in a plume, but act as a source of NO_x in rural

and remote regions (Finlayson-Pitts and Pitts, 1999). In addition, the non-linear interactions between NO_x and OH make the lifetime of NO_x in a fresh plume very different from its lifetime several hours downwind (e.g. Martinez et al., 2003; Valin et al., 2013).

To constrain the lifetime of NO_x in rural and remote regions, observations of reactive nitrogen species must be combined with an understanding of the chemical transformations between NO_x and its higher oxides. If the production, loss, and fate of these higher oxides are accurately understood, then the lifetime of NO_x can be calculated by tracing the flow of reactive nitrogen through the system. Here, we evaluate the daytime lifetime of NO_x in the rural southeast United States, using measurements taken from 1 June – 15 July 2013 as part of the Southern Oxidant and Aerosol Study (SOAS). In-situ measurements of Volatile Organic Compounds (VOCs), atmospheric oxidants, and a wide range of reactive nitrogen compounds are used to determine the production and loss rates for nitric acid, alkyl and multifunctional nitrates, and peroxy nitrates. These rates are used to assess the lifetime of NO_x in this region.

2   The NO_y family and the lifetime of NO_x

During the day, NO_x is lost by associating with other radicals to produce higher oxides of nitrogen, primarily nitric acid, alkyl and multifunctional nitrates ($\Sigma ANs = \Sigma RONO_2$), and peroxy nitrates ($\Sigma PNs = \Sigma R(O)OONO_2$) (e.g. Day et al., 2003; Perring et al., 2010). The sum of these and other higher oxides such as N_2O_5 and HONO are collectively known as NO_z ($NO_z \equiv NO_y - NO_x$).

NO_x is oxidized to produce the major daytime classes of NO_z through reactions (R1), (R2b), and (R3).

$$NO_2 + OH + M \rightarrow HNO_3 + M \tag{R1}$$

$$NO + RO_2 + M \rightarrow RONO_2 + M \tag{R2b}$$

$$NO_2 + R(O)O_2 + M \rightleftharpoons R(O)OONO_2 + M \tag{R3}$$

NO_x can also be converted to NO_z through reactions of the NO_3 radical. Although these reactions are most important at night, previous studies have shown that NO_3 chemistry can produce NO_z during the day if concentrations of alkenes are high (e.g. Fuentes et al., 2007; Mogensen et al., 2015; Ayres et al., 2015).

The production and fate of different NO_z species determine the lifetime of NO_x. Some of these species are short-lived and re-release NO_x back to the atmosphere within hours of being formed. If the lifetime for the conversion of a NO_z species back to NO_x is shorter than typical NO_x lifetimes in the atmosphere, then NO_x and these NO_z species interact, and their concentrations will approach a steady-state ratio. As NO_x is removed from the system, some of the short-lived NO_z species dissociate, buffering the concentration of NO_x. In this way, the presence of NO_x reservoirs directly extends the lifetime of NO_x.

One method to take this buffering into account when calculating the lifetime of NO_x is to consider the sum of NO_x and all NO_z species with lifetimes to re-release of NO_x shorter than the atmospheric lifetime of NO_x. We define this sum as short-lived reactive nitrogen, or NO_{SL}. The remaining forms of reactive nitrogen are defined as long-lived reactive nitrogen (NO_{LL}). The division between NO_{SL} and NO_{LL} depends on the lifetime of NO_x. For the initial discussion in this manuscript, we use a provisional lifetime of 7 hours to divide NO_z species between NO_{SL} and NO_{LL}. This cutoff is in the middle of the range of NO_x lifetimes found in plume studies (e.g. Ryerson et al., 1998; Dillon et al., 2003; Alvarado et al., 2010; Valin et al., 2013). The provisional cutoff chosen as a starting point does not affect the final results.

In areas well removed from large NO_x sources, NO_x and its short-lived reservoirs interconvert significantly faster than the rate of change of NO_x. Under these conditions, the lifetime of $NO_x (\tau_{NO_x})$ is equal to the lifetime of NO_{SL}. If the conversion of NO_{LL} to NO_{SL} is negligible, then the lifetime of NO_x can be calculated by Eq. (1):

$$\tau_{NO_x} = \tau_{NO_{SL}} = \frac{[NO_{SL}]}{\mathcal{L}(NO_{SL})} \tag{1}$$

Throughout this paper, we use $\mathcal{L}(X)$ to indicate the gross loss rate of the compound or class of compounds X.

The relationship and interactions between NO_{SL} and NO_{LL}, and their typical compositions in the planetary boundary layer, are shown in Fig. 1. In the summertime at midlatitudes, peroxy nitrates typically release NO_x within hours of being formed (LaFranchi et al., 2009), making them a component of NO_{SL}. Under these same conditions, nitric acid typically converts back to NO_x on timescales of 100 hours or greater (Finlayson-Pitts and Pitts, 1999) and is a component of NO_{LL}. The fate and lifetime of ΣANs, the third major component of NO_z, remain poorly understood, making it uncertain whether ΣANs act as a component of NO_{SL} or NO_{LL} (Perring et al., 2013, and references therein). This is especially true for the multifunctional, biogenically-derived nitrates that are the predominant component of ΣANs in forested areas (e.g. Beaver et al., 2012).

Recent studies of multifunctional nitrates suggest that the main daytime loss pathways of these species are deposition, reaction with OH, photolysis, and heterogeneous hydrolysis to produce nitric acid (e.g. Darer et al., 2011; Browne et al., 2013; Lee et al., 2014; Müller et al., 2014; Lee et al., 2016; Nguyen et al., 2015). These recent studies, combined with the extensive measurements made during SOAS, allow us to provide new constraints on the lifetime and fate of ΣANs and therefore to more accurately determine the lifetime of NO_x.

3   Instrumentation and measurements

The primary ground site for SOAS was located in Bibb County, Alabama (32.90289° N, 87.24968° W) at the Centreville (CTR) long-term monitoring site in the SouthEastern Aerosol Research and CHaracterization (SEARCH) Network (Hansen et al., 2003). This location is 40 km southeast of Tuscaloosa (population 95,000), and 90 km southwest of Birmingham (population 210,000). Comparison with long-term measurements indicate that the summer of 2013 was cooler and cloudier than typical for previous summers (Hidy et al., 2014). Gas-phase measurements used in this study were located on a 20 m walk-up tower at the edge of the forest. Nitrate ion and meteorological parameters were measured in a clearing approximately 50 m away from the tower.

A nearly complete suite of reactive nitrogen species, including NO, NO_2, ΣPNs, ΣANs, HNO_3, and NO_3^-, was measured during SOAS. NO was measured using the chemiluminescence instrument described in Min et al. (2014). The reaction of ambient NO with added excess O_3 formed excited NO_2^* molecules. A fraction of these fluoresce, and the emitted photons were collected on a red-sensitive photomultiplier tube (Hamamatsu H7421-50). Calibrations were performed every 2 hours by diluting NO standard gas (5.08 ppm $\pm 5\%$ NO in N_2, Praxair) to 3–20 ppb in zero air and adding it to the instrument inlet. The mixing ratio was corrected for enhanced quenching by water vapor (Thornton et al., 2000) using co-located measurements of relative humidity and temperature.

NO_2, ΣPNs, and ΣANs were measured via Thermal Dissociation Laser Induced Fluorescence (TD-LIF), as described by Day et al. (2002). Ambient air was drawn into a multipass White cell, where a 532 nm Nd-YAG laser excited the NO_2 molecules, and their fluorescence signal was collected on a photomultiplier tube (Hamamatsu H7421-50). The same instrument was used to measure the sum of peroxy nitrates and the sum of alkyl and multifunctional nitrates by first passing the air through a heated oven, where the organic nitrates dissociated to form NO_2. Organic nitrates present in the particle phase undergo evaporation and thermal dissociation in the heated ovens to form NO_2. The TD-LIF measurement of ΣANs therefore includes alkyl and multifunctional nitrates in both the gas and particle phases, but does not include HNO_3 or particle-phase inorganic nitrate (Day et al., 2002; Rollins et al., 2010). All of the channels were calibrated by injecting NO_2 standard gas (5.03 ppm $\pm 5\%$ NO_2 in N_2, Praxair) and corrected for enhanced quenching by water vapor.

Nitric acid was measured in the gas phase by chemical ionization mass spectrometry (CIMS), using CF_3O^- as the reagent ion (Crounse et al., 2006). The ions were quantified using a compact time-of-flight mass spectrometer, and the instrument was calibrated in the field using isotopically labeled nitric acid. Particle-phase inorganic nitrate (NO_3^-) was measured using a Monitor for AeRosols and GAses (MARGA) (Allen et al., 2015). Ambient air was drawn through a rotating wet-walled denuder which collected water soluble gas-phase compounds. Particle-phase compounds were captured by a steam-jet aerosol collector downstream of the denuder. Water soluble ions from both phases were then quantified via ion chromatography. This measurement of NO_3^- is designed to be specific to inorganic nitrate, and is not affected by ΣANs in the particle phase (Allen et al., 2015).

Measurements of reactive nitrogen species are summarized in Fig. 2. Concentrations of NO_{SL} compounds (NO, NO_2, and ΣPNs) are shown in Fig. 2a. Afternoon concentrations of NO_2 and NO were typically around 220 ppt and 50 ppt respectively. After sunset, NO dropped to near zero, and NO_2 began to increase. At sunrise, NO concentrations rapidly rose to over 200 ppt between 6 am and 8 am Central Standard Time (CST) while NO_2 decreased sharply. By 11 am, when the daytime boundary layer was well developed, the concentrations of NO and NO_2 returned to their typical afternoon values. Concentrations of ΣPNs were 160 ppt at sunrise, increased to a maximum concentration of 300 ppt at 9 am and declined slowly throughout the rest of the day.

Concentrations of HNO_3 and inorganic NO_3^-, components of NO_{LL}, are shown in Fig. 2b. Both species increased slowly after sunrise and reached a maximum combined concentration of 300 ppt at 1 pm, before declining to a combined concentration of 175 ppt at night. The total concentration of ΣANs in both the gas and particle phase, whose partitioning into NO_{SL} and

NO_{LL} is not known, are shown in Fig. 2c. ΣANs averaged 150 ppt during the night and increased sharply after sunrise. After reaching a maximum of 250 ppt at 8 am, ΣANs declined slowly to a minimum concentration of 125 ppt at sunset.

OH, HO_2, and OH Reactivity (OHR) were measured via Fluorescence Assay by Gas Expansion (FAGE) of OH. A 308 nm dye laser excited the OH radicals and their fluorescence was detected by an electronically gated microchannel plate detector (Faloona et al., 2004). Calibration of the system was performed by in-situ generation of OH radicals via photolysis of water vapor. Chemical zeroing was performed by periodically adding C_3F_6 to the sampling inlet in order to quantify the interference from internally generated OH observed in previous field campaigns (Mao et al., 2012). HO_2 was measured in a second channel by adding NO to chemically convert HO_2 to OH. The amount of added NO was regulated such that HO_2 but not RO_2 was converted to OH (Fuchs et al., 2011). Total OH Reactivity (OHR) was measured by drawing ambient air through a flow tube and mixing it with a fixed concentration of OH. At the end of the flow tube, the concentration of OH was measured. The OH Reactivity is determined by the slope of the OH signal versus reaction time (Mao et al., 2009).

Measured concentrations of OH peaked at 0.045 ppt and concentrations of HO_2 at 30 ppt during SOAS (Fig. 3, top panel). Both OH and HO_2 increased slowly throughout the morning and reached their maximum in the early afternoon. Concentrations then fell as the sun set, with OH usually dropping below 0.01 ppt by 7 pm. The measured OH Reactivity was high, reaching an afternoon peak of close to 25 s^{-1} (Fig. 3, bottom panel). OHR decreased throughout the night, reaching a minimum of 10 s^{-1} just before sunrise.

Measurements of ozone were made using a Cavity Ring Down Spectrometer (Washenfelder et al., 2011). O_3 is chemically converted to NO_2 by reaction with excess NO, and the resulting NO_2 is measured by cavity ring-down spectroscopy at 404 nm. The concentration of ozone increased from a minimum of 15 ppb at sunrise to a maximum of 38 ppb in the late afternoon (Fig. 3, middle panel).

Volatile organic compounds were measured primarily by Gas Chromatography - Mass Spectrometry (GC-MS). Samples were collected in a liquid-nitrogen cooled trap for five minutes, and then transferred by heating onto an analytical column, and detected using an electron-impact quadrupole mass-spectrometer (Goldan et al., 2004; Gilman et al., 2010). This system was able to quantify a wide range of compounds including alkanes, alkenes, aromatics, isoprene, and multiple monoterpenes. The sum of methyl vinyl ketone (MVK) and methacrolein (MACR) was measured using a Proton Transfer Reaction - Time of Flight - Mass Spectrometer (PTR-TOF-MS) (Kaser et al., 2013). The interference in this measurement from the decomposition of isoprene hydroperoxides on instrument inlets (Rivera-Rios et al., 2014) is not corrected for, and increases the uncertainty in this measurement by approximately 20%.

VOC measurements at the site show that the OHR was dominated by reaction with biogenic compounds. Figure 3 shows the OH Reactivity of individually measured compounds as a stacked area plot. In the daytime, isoprene accounted for nearly half of the total reactivity, while VOCs typically attributed to anthropogenic activities, including alkanes, aromatics, and simple alkenes, were responsible for less than 10% of the measured OHR. Not included in Fig. 3 is the reactivity of VOCs whose reaction with OH does not lead to net loss of OH, and therefore does not contribute to the measured OHR. These compounds, primarily isoprene hydroperoxides (ISOPOOH) and C5-hydroxyaldehydes (HPALD), have an average daytime reactivity of 2 s^{-1}. The sum of individual reactivities shows a similar diurnal pattern to the measured OHR, and accounts for 70–85% of the

total. Unknown biogenic emissions, small aldehydes and alcohols, and other 2nd and 3rd generation VOC oxidation products are all possible contributors to the missing reactivity (e.g. Di Carlo et al., 2004; Goldstein and Galbally, 2007; Pusede et al., 2014; Kaiser et al., 2016). Meteorological parameters including temperature and solar radiation were measured by Atmospheric Research and Analysis as part of SEARCH.

4 The production and loss of individual NO_x reservoirs

4.1 Nitric acid

In the boundary layer, the production of nitric acid is typically followed by deposition and thus leads to the permanent removal of reactive nitrogen from the atmosphere. Nitric acid can undergo photolysis or reaction with OH to produce NO_x, but these processes are slow (Burkholder et al., 1993; Atkinson et al., 2006), with an average calculated rate during SOAS of less than 0.2 ppt hr^{-1}. Gas-phase nitric acid can also partition into aerosols. Nitric acid is long lived in the particle phase and is typically lost by re-evaporation into the gas phase (e.g. Hennigan et al., 2008). The loss of nitric acid through deposition of aerosols is typically negligible compared to its gas-phase deposition (e.g. Zalakeviciute et al., 2012). Because nitric acid releases NO_x so slowly, it is a component of NO_{LL}.

The deposition velocity (v_{dep}) of HNO_3 in the gas phase was measured during SOAS by Nguyen et al. (2015). Around midday, when the boundary layer is well developed, the deposition velocity can be combined with the boundary layer height (BLH) to calculate a loss rate of HNO_3:

$$\mathcal{L}(HNO_3) = \frac{v_{dep}}{BLH} \cdot [HNO_3] \qquad (2)$$

Using this method, we find the lifetime of nitric acid in the gas and particle phase to be 6 hours at noon. In the late afternoon, changing boundary layer dynamics make this calculation of the loss rate inaccurate (e.g. Papale et al., 2006; Millet et al., 2015). The loss of nitric acid in the late afternoon was therefore calculated by fitting periods of consistent decay between 3 pm and 7 pm with an exponential curve. By fitting only the periods of consistent decay, we aim to select for periods where the production of nitric acid is at a minimum and the observed net decay of nitric acid is similar to its gross loss rate. Because nitric acid reversibly partitions between the gas and particle phases, the lifetime was calculated based on the concentration of nitric acid in both phases. The lifetime calculated using this method is 5^{+3}_{-2} hours, similar to the lifetime of nitric acid calculated using Eq. 2 at noon.

By combining the loss rate of nitric acid with the rate of change of its concentration, we can calculate an inferred production rate of nitric acid (Fig. 4). This inferred production rate for each hour is defined as the difference between the rate of change in the concentration of nitric acid and the loss rate. The rate of change was determined as the slope of a best-fit line of the concentration of nitric acid versus time for each hour.

Since the calculation of the inferred production rate considers only the hour-to-hour change in nitric acid and not its gross concentration, the inferred production rate is not affected by distant nitric acid sources. We find very small (less than 15%) variation in the concentration of NO_x with wind direction and no correlation of the inferred production rate around noon

with sulfate (a power plant tracer) or benzene (an urban tracer). As the transport time from these sources to the CTR site is significantly greater than 1 hour, this result is not surprising. The changing boundary layer height could significantly impact the inferred production rate of nitric acid during the early morning, but it is likely unimportant at midday.

Also shown in Fig. 4 is the rate of nitric acid production from the reaction of $OH + NO_2$ (R1), using the rate constant measured by Mollner et al. (2010). The vertical bars for the inferred rate represent the combined effects of the uncertainty in both the fit of concentration v. time and in the calculated nitric acid lifetime, as well as the day-to-day variations in the observations. The vertical bars shown for the production of nitric acid from the $OH + NO_2$ reaction include both the systematic and random errors in the measurements of OH and NO_2 and in the rate coefficient, k_{OH+NO_2}, combined in quadrature.

Between 10 am and 2 pm, when photochemistry is most active, the inferred production rate is 3–4 times larger than the rate of reaction (R1), a difference of approximately 30 ppt hr^{-1}. The most likely explanation for the missing nitric acid production during this time is the heterogeneous hydrolysis of ΣANs. This has been proposed as an important source of nitric acid over the Canadian boreal forest (Browne et al., 2013), and the hydrolysis of tertiary alkyl nitrates on atmospherically relevant timescales has been observed in several laboratory experiments (e.g. Darer et al., 2011; Liu et al., 2012; Rindelaub et al., 2015). If ΣANs are being converted to nitric acid, this process should appear as a sink in the budget of ΣANs. If other processes are responsible for the missing nitric acid source, these would not affect the budget of ΣANs. Only the conversion of ΣANs to nitric acid will lead to a missing source of nitric acid and a missing sink of ΣANs.

4.2   Alkyl and multifunctional nitrates

Previous observational studies have found that the production of ΣANs is rapid in forested regions (e.g. Day et al., 2009; Beaver et al., 2012; Fry et al., 2013; Browne et al., 2013), but the subsequent fates of these biogenic nitrates are not well constrained. During the day, ΣANs are produced primarily from the reaction of organic peroxy radicals (RO_2) with NO. Most of the time, this leads to the formation of RO and NO_2 (R2a), but a fraction of the time produces an organic nitrate (R2b). The branching ratio $k_{R2b}/(k_{R2b} + k_{R2a})$ is designated α and varies with the structure of the R group, as well as the temperature and pressure.

$$NO + RO_2 \rightarrow RO + NO_2 \tag{R2a}$$

$$NO + RO_2 + M \rightarrow RONO_2 + M \tag{R2b}$$

Organic peroxy radicals are produced in the daytime troposphere predominantly by the reaction of OH with VOCs and are lost through reaction with NO, HO_2, and RO_2, or through unimolecular isomerization. These radicals reach steady state within seconds, allowing the production of ΣANs via reaction (R2b) to be calculated as:

$$P(\Sigma ANs) = \sum_{R_i} \alpha_i \cdot f_{NO_i} \cdot k_{OH+R_i} \cdot [R_i] \cdot [OH] \tag{3}$$

The value f_{NO} represents the fraction of RO_2 radicals that are lost by reaction with NO. This value was calculated separately for each measured VOC and is equal to the rate of reactions R2b and R2a, divided by the sum of all RO_2 loss rates. Rate constants for the reaction of RO_2 radicals with NO, HO_2, and other RO_2 radicals are taken from the Master Chemical Mechanism v3.2 (Saunders et al., 2003) for all species other than isoprene and methacrolein. The reactions of isoprene-derived RO_2 radicals are based on the LIM-1 scheme described by Peeters et al. (2014), with the rate of unimolecular isomerization scaled to match the rate of HPALD formation observed in chamber experiments by Crounse et al. (2011). For methacrolein, we include the isomerization rate described by Crounse et al. (2012). Unimolecular isomerization is not included for any other RO_2 species. Concentrations of RO_2 radicals are calculated iteratively at each point until they converge.

Values of k_{OH+R_i} and α_i are taken from Atkinson and Arey (2003) and Perring et al. (2013) respectively, with the following exceptions. An α of 0.26 is used for α-pinene, following Rindelaub et al. (2015). An α of 0.12 is used for isoprene. This is in the middle of the range of branching ratios for isoprene (0.09–0.15) found in recent experiments (e.g. Paulot et al., 2009; Teng et al., 2015; Xiong et al., 2015).

The missing OH Reactivity (Fig. 3) is included in this calculation as a generic VOC that forms RO_2 radicals that react with the same kinetics as $CH_3CH_2O_2$. This is an appropriate value if the missing reactivity is composed of small or highly oxygenated compounds (Perring et al., 2013). If the missing VOC Reactivity has a significant contribution from large hydrocarbons, then this value should be higher.

The daytime production of ΣANs also includes a minor contribution from the reaction of NO_3 with alkenes, via reactions (R4) and (R5).

$$NO_2 + O_3 \rightarrow NO_3 + O_2 \tag{R4}$$

$$NO_3 + R \rightarrow RONO_2 \tag{R5}$$

Concentrations of isoprene and monoterpenes were sufficiently elevated during SOAS that reaction with these compounds is a significant fraction of the total daytime loss of NO_3. Calculations following Ayres et al. (2015) indicate that this pathway produces ΣANs at an average rate of 10 ppt hr^{-1}.

The calculated total rate of ΣAN production via (R2b) and (R5) is rapid, averaging approximately 90 ppt hr^{-1} between 8 am and 4 pm (Fig. 5). The oxidation of isoprene accounts for over three-quarters of the production of ΣANs, and monoterpenes account for an additional 15%. Based on the uncertainty in each term in Eq. 3, the total systematic uncertainty in the production rate of ΣANs is estimated to be $\pm 50\%$ (one sigma). The largest contribution to the total uncertainty comes from the calculation of f_{NO} for isoprene. Reported uncertainties for the rate constants and radical concentrations involved in RO_2 loss (Boyd et al., 2003; Ghosh et al., 2010; Crounse et al., 2011; Peeters et al., 2014) combine to give an overall uncertainty of $\pm 35\%$ in f_{NO} for isoprene. Uncertainty in the values of alpha and the nature of the missing VOCR are also significant contributions to the total uncertainty. The effects of boundary layer growth are not accounted for, but are unlikely to be important after 10 am (e.g. Xiong et al., 2015). The 55% uncertainty constrains the average ΣANs production rate to between 50 and 145 ppt hr^{-1}.

Rapid production of ΣANs decreases the NO_x lifetime only if it leads to the long-term removal of NO_x from the atmosphere. This can occur either if the alkyl and multifunctional nitrates produced are themselves long lived, or if they have short lifetimes but are lost primarily to deposition or to conversion to a different NO_z species that is long-lived. Despite rapid production of ΣANs during the day, the diurnal cycle of ΣANs exhibits a decrease between 9 am and 7 pm (Fig. 2c), implying that the ΣANs loss rate must be rapid.

While ΣANs do not build up over the course of a day, their concentration is strongly correlated with their instantaneous production rate in the afternoon (Fig. 6). We interpret these two results to indicate that ΣANs are short-lived and near steady-state in the afternoon. A least-squares fit between ΣAN production and concentration gives a slope of 1.7 hours and an intercept of 40 ppt. If ΣANs are near steady-state, then the slope of this correlation is equal to the ΣAN lifetime. The intercept of 40 ppt is interpreted as the large-scale background of long-lived ΣANs during summertime at mid-latitudes. This background is likely composed of small monofunctional alkyl nitrates, since these compounds typically have lifetimes of days or weeks in the summertime troposphere (e.g Clemitshaw et al., 1997). Ethyl and isopropyl nitrate were measured by GC-MS during SOAS, and show a consistent concentration of $\sim$20 ppt, explaining 50% of the intercept. Previous observations over North America suggest that the summed concentration of small monofunctional nitrates not measured during SOAS is likely also around 20 ppt in the southeast United States, accounting for the other 50% (e.g. Schneider et al., 1998; Blake et al., 2003; Russo et al., 2010).

A lifetime of 1.7 hours for the reactive component of ΣANs is roughly consistent with previous estimates. Perring et al. (2009) found a lifetime of 1.5–2.5 hr for ΣANs in the southeast United States, based on the correlation between ΣANs and formaldehyde. Multiple studies have also found evidence for rapid loss of ΣANs through particle-phase processing in the southeast United States (e.g. Lee et al., 2016; Pye et al., 2015). This reactive component is likely composed of larger, multi-functional nitrates that can be lost rapidly by oxidation, deposition, or hydrolysis (Lee et al., 2014; Nguyen et al., 2015; Darer et al., 2011).

Because most ΣANs are short-lived, they do not serve as a permanent sink of NO_x directly. To establish whether ΣANs are a component of NO_{SL} or NO_{LL}, the fate of ΣANs must be understood. Conversion of an alkyl nitrate to another alkyl nitrate does not affect the measurement of ΣANs and therefore does not contribute to the calculated 1.7 hour lifetime. The only other NO_y compounds produced by alkyl nitrate oxidation that have been observed in laboratory experiments are NO_x and nitric acid (e.g. Lee et al., 2014; Darer et al., 2011). These two products are thought to arise from completely different mechanisms in the oxidation of ΣANs. NO_x is produced either during the gas-phase oxidation of nitrates (Lee et al., 2014) or by the photolysis of carbonyl nitrates (Müller et al., 2014), while nitric acid is produced only by the heterogeneous hydrolysis of hydroxy-nitrates (Darer et al., 2011). The question of whether ΣAN to nitric acid conversion is occurring is therefore equivalent to the question of whether deposition and the sum of all gas-phase loss processes are sufficient to explain the 1.7 hr lifetime of ΣANs. If these processes cannot explain the short lifetime of ΣANs, then the unaccounted-for loss is likely due to heterogeneous formation of nitric acid.

An upper limit to the gas-phase oxidation rate of ΣANs can be calculated using measurements of ΣANs by assuming that all alkyl and multifunctional nitrates react with OH and O_3 at the same rate as isoprene hydroxy-nitrates and that these reactions

all lead to loss of ΣANs. Over three-quarters of the ΣANs produced during SOAS were isoprene hydroxy-nitrates (Fig. 5), making the average loss rate of ΣANs close to the rate for isoprene hydroxy-nitrates. In addition, under low-NO_x conditions, the most likely products of ΣAN oxidation are either NO_x or carbonyl nitrates (Lee et al., 2014). Studies by Müller et al. (2014) and Xiong et al. (2016) indicate that carbonyl nitrates are rapidly photolyzed to release NO_x. If the photolysis rate is fast enough, then it is a reasonable approximation to treat ΣANs as releasing NO_x every time they are oxidized.

Only ΣANs present in the gas phase are likely to undergo deposition or reaction with OH or O_3. Observations during SOAS indicate that 20% of ΣANs may be in the particle phase during the afternoon (Lee et al., 2016); however, even if we assume that all ΣANs are gas-phase, the rate of gas-phase oxidation plus the rate of deposition measured by Nguyen et al. (2015) during SOAS is insufficient to explain the loss of ΣANs in the afternoon (Fig. 7, filled areas). Since isoprene hydroxy-nitrates and most other first-generation nitrates must be further oxidized before undergoing photolysis, we do not include photolysis as a separate loss process in Fig. 7. Nitrates produced in the oxidation of compounds such as MVK and MACR can undergo photolysis without reacting with OH first, but these are a minor fraction of the total ΣAN production rate (Fig. 5).

If the gap between the individual loss processes and the overall loss rate of ΣANs is attributed entirely to ΣAN hydrolysis, then the rate of nitric acid production from ΣANs would be 65 ppt hr^{-1}. This is two-thirds of the total ΣAN production rate, and roughly equal to the calculated production rate of tertiary nitrates (Peeters et al., 2014; Rindelaub et al., 2015). Laboratory experiments have shown that, in general, tertiary nitrates undergo hydrolysis far faster than primary or secondary nitrates (Darer et al., 2011; Hu et al., 2011), making it likely that the rate of ΣAN hydrolysis is similar to the rate of tertiary ΣAN production.

While the simultaneous presence of a significant missing source of nitric acid and a missing sink of ΣANs supports the idea that ΣAN to nitric acid conversion is occurring, the missing sink of ΣANs is approximately a factor of two larger than the missing source of nitric acid (Fig. 7, hatched area). The discrepancy between the two calculations of the ΣAN hydrolysis rate could be accounted for by uncertainty in the measurements, in the calculated production rate of ΣANs, or in the calculated lifetime of nitric acid. As the data from SOAS is insufficient to determine which of these interpretations is correct, we use the average of the missing nitric acid production rate and the missing ΣAN loss rate as our best estimate of the ΣAN hydrolysis rate.

Using this average, the rate of ΣAN hydrolysis to produce nitric acid is 45 ppt hr^{-1} between 10 am and 2 pm. When this is combined with the loss of ΣANs by deposition, 55% of the ΣANs produced lead to the permanent removal of NO_x from the atmosphere. Using the hydrolysis rate calculated from only the nitric acid budget or only the ΣANs budget changes this fraction to 35 or 75%. The remaining locally produced ΣANs are assumed to re-release NO_x back to the atmosphere through oxidation and photolysis.

Based on the lifetime and fate calculated here, locally-produced ΣANs have a lifetime to re-release of NO_x of just under 4 hours, making them part of NO_{SL}. At the same time, deposition and the rapid conversion of reactive multifunctional nitrates to nitric acid means that the formation of ΣANs leads to the significant removal of NO_{SL}, and therefore NO_x, from the atmosphere.

4.3 Peroxy nitrates

Peroxy nitrates are produced through the association of a peroxy acyl radical with NO_2 (R3). While non-acyl peroxy radicals can also associate with NO_2, the product is extremely unstable and decomposes within seconds in the summertime boundary layer. Peroxy nitrates are primarily lost by thermal dissociation to form NO_2 and a peroxy acyl radical. This acyl radical can either react with NO_2 to reform a peroxy nitrate, or react with NO or HO_2 to form an acyloxy radical or a peracid. The lifetime of peroxy nitrates therefore depends on the temperature and the relative concentrations of NO_2, NO, and HO_2 (LaFranchi et al., 2009). Rate constants from Orlando and Tyndall (2012) and Atkinson et al. (2006) for the reactions of peroxy acyl nitrate and acyl peroxy radical were used to calculate the lifetime of peroxy nitrates during SOAS.

During the day, peroxy nitrates re-release NO_x on timescales of 1–2 hours and are a component of NO_{SL}. The production of peroxy nitrates therefore does not contribute to the net loss of NO_{SL}, but still affects the lifetime of NO_{SL} by adjusting the amount of NO_x available for reactions that produce ΣANs or nitric acid. At SOAS, the ratio of peroxy nitrates to NO_x is typically around 0.7 at midday.

There are other loss processes of peroxy nitrates. The reaction of OH with methacryloyl peroxy nitrate (MPAN) is rapid, but MPAN is typically a minor component of total peroxy nitrates (LaFranchi et al., 2009). The deposition rate of peroxy nitrates was not measured during SOAS, but previous measurements in a ponderosa pine forest estimate the deposition velocity to be between 0.5 and 1.3 cm s^{-1} (Wolfe et al., 2009; Min et al., 2012). Using this range of deposition velocities gives a total deposition loss rate of peroxy nitrates of 5 ± 3 ppt hr^{-1} in the afternoon.

5 The photochemical lifetime of NO_x and NO_{SL}

The measured concentrations and calculated production and loss rates of each individual NO_z species can be combined to determine the lifetime of NO_{SL}. This lifetime depends on the distribution of NO_z between NO_{SL} and NO_{LL} and the chemical transformations between these two classes. If a 7 hour lifetime to re-release of NO_x is used as the provisional dividing line between NO_{SL} and NO_{LL}, then in the afternoon NO_{SL} was composed of NO_x, ΣPNs, and the reactive component of ΣANs. As discussed earlier, both peroxy nitrates and ΣANs have lifetimes to re-release of NO_x of less than 4 hours. During the same time, NO_{LL} was composed of nitric acid and unreactive ΣANs. We interpret the y-intercept in the correlation between ΣAN production and concentration (Fig. 6) to represent a 40 ppt background of unreactive ΣANs, likely composed of small monofunctional nitrates. We treat all ΣANs greater than this constant background as short-lived.

The lifetime of NO_{SL} can then be calculated as $\tau_{NO_{SL}} = [NO_{SL}]/\mathcal{L}(NO_{SL})$. The individual processes that lead to loss of NO_{SL} and their average value between 10 am and 2 pm during SOAS are shown in Fig. 8. The loss of short-lived reactive nitrogen is dominated by the hydrolysis of ΣANs to produce nitric acid. This single process accounts for 65% of the total NO_{SL} loss.

NO_{SL} is also converted to NO_{LL} during SOAS through the association of OH and NO_2 to produce nitric acid and the production of small, unreactive alkyl nitrates. The deposition of both peroxy nitrates and ΣANs, as well as the uptake of NO_x by plants, also leads to the loss of NO_{SL}. Based on the deposition velocity of NO_x over vegetation measured by Breuninger

et al. (2013), the rate of NO_x uptake was calculated to be approximately 1 ppt hr^{-1}. A 50% uncertainty in the ΣAN hydrolysis rate, combined in quadrature with the uncertainties from the other NO_{SL} loss processes, gives the overall uncertainty in the NO_{SL} loss rate of ± 25 ppt hr^{-1}.

When combined with the average concentration of NO_{SL} of 700 ppt during this same time period, the lifetime of NO_{SL}, and therefore the photochemical lifetime of NO_x, is calculated to be 11 ± 5 hours. This calculated lifetime of NO_{SL} is used as the cutoff between NO_{SL} and NO_{LL}. Changing the cutoff from our provisional value of 7 hours to 11 hours does not change the partitioning of NO_y between these two classes.

The long lifetime of NO_x calculated here is qualitatively consistent with the partitioning of NO_y during SOAS. The concentration of NO_{SL} is approximately twice as large as NO_{LL} during the afternoon (Fig. 2). In the absence of large fresh emissions of NO_x, this implies that the conversion of NO_{SL} to NO_{LL} must be slow, in agreement with our calculations. More quantitative calculations of the NO_x lifetime using the ratio of NO_{SL} to NO_{LL} or NO_x to NO_y have been developed for analyses of plumes (e.g. Kleinman et al., 2000; Ryerson et al., 2003) but are not adaptable to this data set.

This NO_x lifetime is longer than the lifetime of NO_x calculated in fresh plumes, where observational studies have found lifetimes of 5–8 hours (e.g. Ryerson et al., 1998; Alvarado et al., 2010; Valin et al., 2013). These studies focus solely on the chemistry of NO_x rather than NO_{SL} and recognition of the buffering effect of organic nitrates would extend the lifetimes found in these studies. In addition, the average noontime concentration of OH observed during SOAS was up to a factor of 5 lower than values typically observed in urban areas (e.g. Mao et al., 2010; Rohrer et al., 2014). Lower concentrations of OH slow the rate of atmospheric oxidation, leading to longer lifetimes of NO_x.

If lower OH and the production of NO_x from peroxy nitrates were the only differences between polluted areas and the regional background, then the lifetime of NO_x during SOAS would be significantly longer than 10 hours. However, the production of ΣANs is extremely rapid and the deposition and hydrolysis of these species accounts for the majority of the NO_x removal in this rural region. The VOC mixture present in the southeast United States leads to very high values of OH Reactivity and α, both of which enhance the production of ΣANs. High concentrations of VOCs also lead to lower OH concentrations and slower production of nitric acid by reaction (R1). Moving from urban centers to rural or remote regions is therefore also a move from nitric acid- to ΣAN-dominated NO_x chemistry. Changes to our understanding of the production and fate of alkyl and multifunctional nitrates will therefore have a large impact on predictions of the lifetime of NO_x and NO_{SL}, with subsequent impacts on the concentration and distribution of NO_x across a region.

6 Conclusions

Measurements in a low-NO_x, high-VOC region provide new insights into the lifetime and chemistry of NO_x and NO_{SL} in rural areas. NO_{SL} is found to have an average lifetime of 11 ± 5 hours, longer than the lifetimes of NO_x observed in plume studies, which do not account for buffering by short-lived NO_z species. The long lifetime of NO_{SL} makes it relatively evenly distributed across the region and allows small inputs of NO_x to sustain the concentrations of NO_{SL} observed during SOAS.

The long daytime lifetime of NO_{SL} found here indicates that NO_x emitted on one day will persist into the night where NO_3 is often the most important oxidant (Brown and Stutz, 2012). Depending the chemistry taking place, NO_{SL} could either be efficiently removed from the atmosphere at night, or remain in the atmosphere until the next day. To fully understand the transport and distribution of NO_x across a region the daytime chemistry of NO_x discussed here must be combined with additional analyses of the nighttime chemistry of NO_x and NO_y (e.g. Brown et al., 2009; Crowley et al., 2011; Ayres et al., 2015).

The production and loss of ΣANs are found to be the most important variables in controlling the lifetime of NO_{SL}. ΣANs were observed to have a lifetime of under 2 hours during the afternoon. This estimate is in line with many previous estimates of ΣAN lifetimes, and indicates that ΣANs are an important short-lived NO_x reservoir. Observations of both nitric acid and ΣANs during SOAS provide strong evidence that both gas-phase oxidation to produce NO_x and particle-phase hydrolysis to produce nitric acid are important chemical loss processes for ΣANs. Comparison of the nitric acid and ΣAN budgets indicate that between 30 and 70% of the alkyl and multifunctional nitrates produced are converted to nitric acid. Further laboratory and field studies are necessary to better constrain this percentage and to understand the mechanisms that control it.

The vast majority of these ΣANs are formed during the oxidation of biogenic hydrocarbons, while much of the NO_x is emitted by anthropogenic activities. In this way, the formation of ΣANs represents an important anthropogenic-biogenic interaction, where the oxidation of biogenic VOCs serves to remove anthropogenic pollution from the atmosphere. In rural and remote regions, the interactions between NO_y, HO_x, and VOCs are complex and bi-directional. As NO_x emissions decrease, ΣANs will likely become an even more important part of the NO_y budget, making it increasingly important that their chemistry and loss be taken into consideration when calculating the lifetime and fate of NO_x.

Acknowledgements. Financial and logistical support for SOAS was provided by the NSF, the Earth Observing Laboratory at the National Center for Atmospheric Research (operated by NSF), the personnel at Atmospheric Research and Analysis, and the Electric Power Research Institute. The Berkeley authors acknowledge the support of the NOAA Office of Global Programs (NA13OAR4310067) and the NSF (AGS-1352972) and by EPA STAR Grant 835407 (to A.H.G.). The Caltech authors acknowledge the support of the NSF (AGS-1331360, AGS-1240604). The Penn State authors acknowledge the support of the NSF (AGS-1246918).

References

Allen, H. M., Draper, D. C., Ayres, B. R., Ault, A., Bondy, A., Takahama, S., Modini, R. L., Baumann, K., Edgerton, E., Knote, C., Laskin, A., Wang, B., and Fry, J. L.: Influence of crustal dust and sea spray supermicron particle concentrations and acidity on inorganic NO_3^- aerosol during the 2013 Southern Oxidant and Aerosol Study, Atmos. Chem. Phys., 15, 10 669–10 685, doi:10.5194/acp-15-10669-2015, 2015.

Alvarado, M. J., Logan, J. A., Mao, J., Apel, E., Riemer, D., Blake, D., Cohen, R. C., Min, K.-E., Perring, A. E., Browne, E. C., Wooldridge, P. J., Diskin, G. S., Sachse, G. W., Fuelberg, H., Sessions, W. R., Harrigan, D. L., Huey, G., Liao, J., Case-Hanks, A., Jimenez, J. L., Cubison, M. J., Vay, S. A., Weinheimer, A. J., Knapp, D. J., Montzka, D. D., Flocke, F. M., Pollack, I. B., Wennberg, P. O., Kurten, A., Crounse, J., St. Clair, J. M., Wisthaler, A., Mikoviny, T., Yantosca, R. M., Carouge, C. C., and Le Sager, P.: Nitrogen oxides and PAN in plumes from boreal fires during ARCTAS-B and their impact on ozone: an integrated analysis of aircraft and satellite observations, Atmos. Chem. Phys., 10, 9739–9760, doi:10.5194/acp-10-9739-2010, 2010.

Atkinson, R. and Arey, J.: Atmospheric Degradation of Volatile Organic Compounds, Chem. Rev., 103, 4605–4638, doi:10.1021/cr0206420, 2003.

Atkinson, R., Baulch, D. L., Cox, R. A., Crowley, J. N., Hampson, R. F., Hynes, R. G., Jenkin, M. E., Rossi, M. J., Troe, J., and IUPAC Subcommittee: Evaluated kinetic and photochemical data for atmospheric chemistry: Volume II – gas phase reactions of organic species, Atmos. Chem. Phys., 6, 3625–4055, doi:10.5194/acp-6-3625-2006, 2006.

Ayres, B. R., Allen, H. M., Draper, D. C., Brown, S. S., Wild, R. J., Jimenez, J. L., Day, D. A., Campuzano-Jost, P., Hu, W., de Gouw, J., Koss, A., Cohen, R. C., Duffey, K. C., Romer, P., Baumann, K., Edgerton, E., Takahama, S., Thornton, J. A., Lee, B. H., Lopez-Hilfiker, F. D., Mohr, C., Wennberg, P. O., Nguyen, T. B., Teng, A., Goldstein, A. H., Olson, K., and Fry, J. L.: Organic nitrate aerosol formation via NO_3 + biogenic volatile organic compounds in the southeastern United States, Atmos. Chem. Phys., 15, 13 377–13 392, doi:10.5194/acp-15-13377-2015, 2015.

Beaver, M. R., St. Clair, J. M., Paulot, F., Spencer, K. M., Crounse, J. D., LaFranchi, B. W., Min, K. E., Pusede, S. E., Wooldridge, P. J., Schade, G. W., Park, C., Cohen, R. C., and Wennberg, P. O.: Importance of biogenic precursors to the budget of organic nitrates: observations of multifunctional organic nitrates by CIMS and TD-LIF during BEARPEX 2009, Atmos. Chem. Phys., 12, 5773–5785, doi:10.5194/acp-12-5773-2012, 2012.

Blake, N. J., Blake, D. R., Sive, B. C., Katzenstein, A. S., Meinardi, S., Wingenter, O. W., Atlas, E. L., Flocke, F., Ridley, B. A., and Rowland, F. S.: The seasonal evolution of NMHCs and light alkyl nitrates at middle to high northern latitudes during TOPSE, J. Geophys. Res., 108, 8359, doi:10.1029/2001JD001467, 2003.

Boyd, A. A., Flaud, P.-M., Daugey, N., and Lesclaux, R.: Rate Constants for RO_2 + HO_2 Reactions Measured under a Large Excess of HO_2, J. Phys. Chem. A, 107, 818–821, doi:10.1021/jp026581r, 2003.

Breuninger, C., Meixner, F. X., and Kesselmeier, J.: Field investigations of nitrogen dioxide (NO_2) exchange between plants and the atmosphere, Atmos. Chem. Phys., 13, 773–790, doi:10.5194/acp-13-773-2013, 2013.

Brown, S. S. and Stutz, J.: Nighttime radical observations and chemistry, Chem. Soc. Rev., 41, 6405–6447, doi:10.1039/C2CS35181A, 2012.

Brown, S. S., Dubé, W. P., Fuchs, H., Ryerson, T. B., Wollny, A. G., Brock, C. A., Bahreini, R., Middlebrook, A. M., Neuman, J. A., Atlas, E., Roberts, J. M., Osthoff, H. D., Trainer, M., Fehsenfeld, F. C., and Ravishankara, A. R.: Reactive uptake coefficients for N_2O_5 determined from aircraft measurements during the Second Texas Air Quality Study: Comparison to current model parameterizations, J. Geophys. Res., 114, D00F10, doi:10.1029/2008JD011679, 2009.

Browne, E. C. and Cohen, R. C.: Effects of biogenic nitrate chemistry on the NO_x lifetime in remote continental regions, Atmos. Chem. Phys., 12, 11 917–11 932, doi:10.5194/acp-12-11917-2012, 2012.

Browne, E. C., Min, K.-E., Wooldridge, P. J., Apel, E., Blake, D. R., Brune, W. H., Cantrell, C. A., Cubison, M. J., Diskin, G. S., Jimenez, J. L., Weinheimer, A. J., Wennberg, P. O., Wisthaler, A., and Cohen, R. C.: Observations of total $RONO_2$ over the boreal forest: NO_x sinks and HNO_3 sources, Atmos. Chem. Phys., 13, 4543–4562, doi:10.5194/acp-13-4543-2013, 2013.

Burkholder, J. B., Talukdar, R. K., Ravishankara, A. R., and Solomon, S.: Temperature dependence of the HNO_3 UV absorption cross sections, J. Geophys. Res.-Atmos., 98, 22 937–22 948, doi:10.1029/93JD02178, 1993.

Clemitshaw, K. C., Williams, J., Rattigan, O. V., Shallcross, D. E., Law, K. S., and Cox, R. A.: Gas-phase ultraviolet absorption cross-sections and atmospheric lifetimes of several C_2–C_5 alkyl nitrates, J. Photochem. Photobio. A, 102, 117–126, doi:10.1016/S1010-6030(96)04458-9, 1997.

Crounse, J. D., McKinney, K. A., Kwan, A. J., and Wennberg, P. O.: Measurement of Gas-Phase Hydroperoxides by Chemical Ionization Mass Spectrometry, Anal. Chem., 78, 6726–6732, doi:10.1021/ac0604235, 2006.

Crounse, J. D., Paulot, F., Kjaergaard, H. G., and Wennberg, P. O.: Peroxy radical isomerization in the oxidation of isoprene, Phys. Chem. Chem. Phys., 13, 13 607–13 613, doi:10.1039/C1CP21330J, 2011.

Crounse, J. D., Knap, H. C., Ørnsø, K. B., Jørgensen, S., Paulot, F., Kjaergaard, H. G., and Wennberg, P. O.: Atmospheric Fate of Methacrolein. 1. Peroxy Radical Isomerization Following Addition of OH and O_2, J. Phys. Chem. A, 116, 5756–5762, doi:10.1021/jp211560u, 2012.

Crowley, J. N., Thieser, J., Tang, M. J., Schuster, G., Bozem, H., Beygi, Z. H., Fischer, H., Diesch, J.-M., Drewnick, F., Borrmann, S., Song, W., Yassaa, N., Williams, J., Pöhler, D., Platt, U., and Lelieveld, J.: Variable lifetimes and loss mechanisms for NO_3 and N_2O_5 during the DOMINO campaign: contrasts between marine, urban and continental air, Atmos. Chem. Phys., 11, 10 853–10 870, doi:10.5194/acp-11-10853-2011, 2011.

Curier, R., Kranenburg, R., Segers, A., Timmermans, R., and Schaap, M.: Synergistic use of OMI NO_2 tropospheric columns and LOTOS–EUROS to evaluate the NO_x emission trends across Europe, Remote Sens. Environ., 149, 58–69, doi:10.1016/j.rse.2014.03.032, 2014.

Dallmann, T. R. and Harley, R. A.: Evaluation of mobile source emission trends in the United States, J. Geophys. Res., 115, D14 305, doi:10.1029/2010JD013862, 2010.

Darer, A. I., Cole-Filipiak, N. C., O'Connor, A. E., and Elrod, M. J.: Formation and Stability of Atmospherically Relevant Isoprene-Derived Organosulfates and Organonitrates, Environ. Sci. Technol., 45, 1895–1902, doi:10.1021/es103797z, 2011.

Day, D. A., Wooldridge, P. J., Dillon, M. B., Thornton, J. A., and Cohen, R. C.: A thermal dissociation laser-induced fluorescence instrument for in situ detection of NO_2, peroxy nitrates, alkyl nitrates, and HNO_3, J. Geophys. Res., 107, 4046, doi:10.1029/2001JD000779, 2002.

Day, D. A., Dillon, M. B., Wooldridge, P. J., Thornton, J. A., Rosen, R. S., Wood, E. C., and Cohen, R. C.: On alkyl nitrates, O_3, and the "missing NO_y", J. Geophys. Res., 108, 4501, doi:10.1029/2003JD003685, 2003.

Day, D. A., Farmer, D. K., Goldstein, A. H., Wooldridge, P. J., Minejima, C., and Cohen, R. C.: Observations of NO_x, ΣPNs, ΣANs, and HNO_3 at a rural site in the California Sierra Nevada Mountains: summertime diurnal cycles, Atmos. Chem. Phys., 9, 4879–4896, doi:10.5194/acp-9-4879-2009, 2009.

Di Carlo, P., Brune, W. H., Martinez, M., Harder, H., Lesher, R., Ren, X., Thornberry, T., Carroll, M. A., Young, V., Shepson, P. B., Riemer, D., Apel, E., and Campbell, C.: Missing OH Reactivity in a Forest: Evidence for Unknown Reactive Biogenic VOCs, Science, 304, 722–725, doi:10.1126/science.1094392, 2004.

Dillon, M. B., Lamanna, M. S., Schade, G. W., Goldstein, A. H., and Cohen, R. C.: Chemical evolution of the Sacramento urban plume: Transport and oxidation, J. Geophys. Res.-Atmos., 107, 4045, doi:10.1029/2001JD000969, 2003.

Faloona, I. C., Tan, D., Lesher, R. L., Hazen, N. L., Frame, C. L., Simpas, J. B., Harder, H., Martinez, M., Di Carlo, P., Ren, X., and Brune, W. H.: A Laser-induced Fluorescence Instrument for Detecting Tropospheric OH and HO_2: Characteristics and Calibration, J. Atmos. Chem., 47, 139–167, doi:10.1023/B:JOCH.0000021036.53185.0e, 2004.

Finlayson-Pitts, B. and Pitts, J.: Chemistry of the Upper and Lower Atmosphere: Theory, Experiments, and Applications, Elsevier Science, San Diego, 1999.

Fowler, D., Coyle, M., Skiba, U., Sutton, M. A., Cape, J. N., Reis, S., Sheppard, L. J., Jenkins, A., Grizzetti, B., Galloway, J. N., Vitousek, P., Leach, A., Bouwman, A. F., Butterbach-Bahl, K., Dentener, F., Stevenson, D., Amann, M., and Voss, M.: The global nitrogen cycle in the twenty-first century, Philos. T. Roy. Soc. B, 368, doi:10.1098/rstb.2013.0164, 2013.

Fry, J. L., Draper, D. C., Zarzana, K. J., Campuzano-Jost, P., Day, D. A., Jimenez, J. L., Brown, S. S., Cohen, R. C., Kaser, L., Hansel, A., Cappellin, L., Karl, T., Hodzic Roux, A., Turnipseed, A., Cantrell, C., Lefer, B. L., and Grossberg, N.: Observations of gas- and aerosol-phase organic nitrates at BEACHON-RoMBAS 2011, Atmos. Chem. Phys., 13, 8585–8605, doi:10.5194/acp-13-8585-2013, 2013.

Fuchs, H., Bohn, B., Hofzumahaus, A., Holland, F., Lu, K. D., Nehr, S., Rohrer, F., and Wahner, A.: Detection of HO_2 by laser-induced fluorescence: calibration and interferences from RO_2 radicals, Atmos. Meas. Tech., 4, 1209–1225, doi:10.5194/amt-4-1209-2011, 2011.

Fuentes, J. D., Wang, D., Bowling, D. R., Potosnak, M., Monson, R. K., Goliff, W. S., and Stockwell, W. R.: Biogenic Hydrocarbon Chemistry within and Above a Mixed Deciduous Forest, J. Atmos. Chem., 56, 165–185, doi:10.1007/s10874-006-9048-4, 2007.

Ghosh, B., Bugarin, A., Connell, B. T., and North, S. W.: Isomer-Selective Study of the OH-Initiated Oxidation of Isoprene in the Presence of O_2 and NO: 2. The Major OH Addition Channel, J. Phys. Chem. A, 114, 2553–2560, doi:10.1021/jp909052t, 2010.

Gilman, J. B., Burkhart, J. F., Lerner, B. M., Williams, E. J., Kuster, W. C., Goldan, P. D., Murphy, P. C., Warneke, C., Fowler, C., Montzka, S. A., Miller, B. R., Miller, L., Oltmans, S. J., Ryerson, T. B., Cooper, O. R., Stohl, A., and de Gouw, J. A.: Ozone variability and halogen oxidation within the Arctic and sub-Arctic springtime boundary layer, Atmos. Chem. Phys., 10, 10 223–10 236, doi:10.5194/acp-10-10223-2010, 2010.

Goldan, P. D., Kuster, W. C., Williams, E., Murphy, P. C., Fehsenfeld, F. C., and Meagher, J.: Nonmethane hydrocarbon and oxy hydrocarbon measurements during the 2002 New England Air Quality Study, J. Geophys. Res., 109, D21 309, doi:10.1029/2003JD004455, 2004.

Goldstein, A. H. and Galbally, I. E.: Known and Unexplored Organic Constituents in the Earth's Atmosphere, Environ. Sci. Technol., 41, 1514–1521, doi:10.1021/es072476p, 2007.

Hansen, D. A., Edgerton, E. S., Hartsell, B. E., Jansen, J. J., Kandasamy, N., Hidy, G. M., and Blanchard, C. L.: The Southeastern Aerosol Research and Characterization Study: Part 1—Overview, J. Air Waste Manage., 53, 1460–1471, doi:10.1080/10473289.2003.10466318, 2003.

Hennigan, C. J., Sullivan, A. P., Fountoukis, C. I., Nenes, A., Hecobian, A., Vargas, O., Peltier, R. E., Case Hanks, A. T., Huey, L. G., Lefer, B. L., Russel, A. G., and Weber, R. J.: On the volatility and production mechanisms of newly formed nitrate and water soluble organic aerosol in Mexico City, Atmos. Chem. Phys., 8, 3761–3768, doi:10.5194/acp-8-3761-2008, 2008.

Hidy, G. M., Blanchard, C. L., Baumann, K., Edgerton, E., Tanenbaum, S., Shaw, S., Knipping, E., Tombach, I., Jansen, J., and Walters, J.: Chemical climatology of the southeastern United States, 1999–2013, Atmos. Chem. Phys., 14, 11 893–11 914, doi:10.5194/acp-14-11893-2014, 2014.

Hu, K. S., Darer, A. I., and Elrod, M. J.: Thermodynamics and kinetics of the hydrolysis of atmospherically relevant organonitrates and organosulfates, Atmos. Chem. Phys., 11, 8307–8320, doi:10.5194/acp-11-8307-2011, 2011.

Hudman, R. C., Moore, N. E., Mebust, A. K., Martin, R. V., Russell, A. R., Valin, L. C., and Cohen, R. C.: Steps towards a mechanistic model of global soil nitric oxide emissions: implementation and space based-constraints, Atmos. Chem. Phys., 12, 7779–7795, doi:10.5194/acp-12-7779-2012, 2012.

Ito, A., Sillman, S., and Penner, J. E.: Effects of additional nonmethane volatile organic compounds, organic nitrates, and direct emissions of oxygenated organic species on global tropospheric chemistry, J. Geophys. Res.-Atmos., 112, D06 309, doi:10.1029/2005JD006556, 2007.

Kaiser, J., Skog, K. M., Baumann, K., Bertman, S. B., Brown, S. B., Brune, W. H., Crounse, J. D., de Gouw, J. A., Edgerton, E. S., Feiner, P. A., Goldstein, A. H., Koss, A., Misztal, P. K., Nguyen, T. B., Olson, K. F., St. Clair, J. M., Teng, A. P., Toma, S., Wennberg, P. O., Wild, R. J., Zhang, L., and Keutsch, F. N.: Speciation of OH reactivity above the canopy of an isoprene-dominated forest, Atmos. Chem. Phys. Discuss., in review, doi:10.5194/acp-2015-1006, 2016.

Kaser, L., Karl, T., Schnitzhofer, R., Graus, M., Herdlinger-Blatt, I. S., DiGangi, J. P., Sive, B., Turnipseed, A., Hornbrook, R. S., Zheng, W., Flocke, F. M., Guenther, A., Keutsch, F. N., Apel, E., and Hansel, A.: Comparison of different real time VOC measurement techniques in a ponderosa pine forest, Atmos. Chem. Phys., 13, 2893–2906, doi:10.5194/acp-13-2893-2013, 2013.

Kleinman, L. I., Daum, P. H., Imre, D. G., Lee, J. H., Lee, Y.-N., Nunnermacker, L. J., Springston, S. R., Weinstein-Lloyd, J., and Newman, L.: Ozone production in the New York City urban plume, J. Geophys. Res., 105, 14 495–14 511, doi:10.1029/2000JD900011, 2000.

LaFranchi, B. W., Wolfe, G. M., Thornton, J. A., Harrold, S. A., Browne, E. C., Min, K. E., Wooldridge, P. J., Gilman, J. B., Kuster, W. C., Goldan, P. D., de Gouw, J. A., McKay, M., Goldstein, A. H., Ren, X., Mao, J., and Cohen, R. C.: Closing the peroxy acetyl nitrate budget: observations of acyl peroxy nitrates (PAN, PPN, and MPAN) during BEARPEX 2007, Atmos. Chem. Phys., 9, 7623–7641, doi:10.5194/acp-9-7623-2009, 2009.

Lee, B. H., Mohr, C., Lopez-Hilfiker, F. D., Lutz, A., Hallquist, M., Lee, L., Romer, P., Cohen, R. C., Iyer, S., Kurtén, T., Hu, W., Day, D. A., Campuzano-Jost, P., Jimenez, J. L., Xu, L., Ng, N. L., Guo, H., Weber, R. J., Wild, R. J., Brown, S. S., Koss, A., de Gouw, J., Olson, K., Goldstein, A. H., Seco, R., Kim, S., McAvey, K., Shepson, P. B., Starn, T., Baumann, K., Edgerton, E. S., Liu, J., Shilling, J. E., Miller, D. O., Brune, W., Schobesberger, S., D'Ambro, E. L., and Thornton, J. A.: Highly functionalized organic nitrates in the southeast United States: Contribution to secondary organic aerosol and reactive nitrogen budgets, Proc. Natl. Acad. Sci. USA, 113, 1516–1521, doi:10.1073/pnas.1508108113, 2016.

Lee, L., Teng, A. P., Wennberg, P. O., Crounse, J. D., and Cohen, R. C.: On Rates and Mechanisms of OH and O_3 Reactions with Isoprene-Derived Hydroxy Nitrates, J. Phys. Chem. A, 118, 1622–1637, doi:10.1021/jp4107603, 2014.

Liu, S., Shilling, J. E., Song, C., Hiranuma, N., Zaveri, R. A., and Russell, L. M.: Hydrolysis of Organonitrate Functional Groups in Aerosol Particles, Aerosol Sci. Tech., 46, 1359–1369, doi:10.1080/02786826.2012.716175, 2012.

Mao, J., Ren, X., Brune, W. H., Olson, J. R., Crawford, J. H., Fried, A., Huey, L. G., Cohen, R. C., Heikes, B., Singh, H. B., Blake, D. R., Sachse, G. W., Diskin, G. S., Hall, S. R., and Shetter, R. E.: Airborne measurement of OH reactivity during INTEX-B, Atmos. Chem. Phys., 9, 163–173, doi:10.5194/acp-9-163-2009, 2009.

Mao, J., Ren, X., Chen, S., Brune, W. H., Chen, Z., Martinez, M., Harder, H., Lefer, B., Rappenglück, B., Flynn, J., and Leuchner, M.: Atmospheric oxidation capacity in the summer of Houston 2006: Comparison with summer measurements in other metropolitan studies, Atmos. Environ., 44, 4107–4115, doi:10.1016/j.atmosenv.2009.01.013, 2010.

Mao, J., Ren, X., Zhang, L., Van Duin, D. M., Cohen, R. C., Park, J.-H., Goldstein, A. H., Paulot, F., Beaver, M. R., Crounse, J. D., Wennberg, P. O., DiGangi, J. P., Henry, S. B., Keutsch, F. N., Park, C., Schade, G. W., Wolfe, G. M., Thornton, J. A., and Brune, W. H.: Insights into hydroxyl measurements and atmospheric oxidation in a California forest, Atmos. Chem. Phys., 12, 8009–8020, doi:10.5194/acp-12-8009-2012, 2012.

Mao, J., Paulot, F., Jacob, D. J., Cohen, R. C., Crounse, J. D., Wennberg, P. O., Keller, C. A., Hudman, R. C., Barkley, M. P., and Horowitz, L. W.: Ozone and organic nitrates over the eastern United States: Sensitivity to isoprene chemistry, J. Geophys. Res.-Atmos., 118, 11 256–11 268, doi:10.1002/jgrd.50817, 2013.

Martinez, M., Harder, H., Kovacs, T. A., Simpas, J. B., Bassis, J., Lesher, R., Brune, W. H., Frost, G. J., Williams, E. J., Stroud, C. A., Jobson, B. T., Roberts, J. M., Hall, S. R., Shetter, R. E., Wert, B., Fried, A., Alicke, B., Stutz, J., Young, V. L., White, A. B., and Zamora, R. J.: OH and HO$_2$ concentrations, sources, and loss rates during the Southern Oxidants Study in Nashville, Tennessee, summer 1999, J. Geophys. Res., 108, 4617, doi:10.1029/2003JD003551, 2003.

Mebust, A. K. and Cohen, R. C.: Space-based observations of fire NO$_x$ emission coefficients: a global biome-scale comparison, Atmos. Chem. Phys., 14, 2509–2524, doi:10.5194/acp-14-2509-2014, 2014.

Millet, D. B., Baasandorj, M., Farmer, D. K., Thornton, J. A., Baumann, K., Brophy, P., Chaliyakunnel, S., de Gouw, J. A., Graus, M., Hu, L., Koss, A., Lee, B. H., Lopez-Hilfiker, F. D., Neuman, J. A., Paulot, F., Peischl, J., Pollack, I. B., Ryerson, T. B., Warneke, C., Williams, B. J., and Xu, J.: A large and ubiquitous source of atmospheric formic acid, Atmos. Chem. Phys., 15, 6283–6304, doi:10.5194/acp-15-6283-2015, 2015.

Min, K.-E., Pusede, S. E., Browne, E. C., LaFranchi, B. W., Wooldridge, P. J., Wolfe, G. M., Harrold, S. A., Thornton, J. A., and Cohen, R. C.: Observations of atmosphere-biosphere exchange of total and speciated peroxynitrates: nitrogen fluxes and biogenic sources of peroxynitrates, Atmos. Chem. Phys., 12, 9763–9773, doi:10.5194/acp-12-9763-2012, 2012.

Min, K.-E., Pusede, S. E., Browne, E. C., LaFranchi, B. W., and Cohen, R. C.: Eddy covariance fluxes and vertical concentration gradient measurements of NO and NO$_2$ over a ponderosa pine ecosystem: observational evidence for within-canopy chemical removal of NO$_x$, Atmos. Chem. Phys., 14, 5495–5512, doi:10.5194/acp-14-5495-2014, 2014.

Mogensen, D., Gierens, R., Crowley, J. N., Keronen, P., Smolander, S., Sogachev, A., Nölscher, A. C., Zhou, L., Kulmala, M., Tang, M. J., Williams, J., and Boy, M.: Simulations of atmospheric OH, O$_3$ and NO$_3$ reactivities within and above the boreal forest, Atmos. Chem. Phys., 15, 3909–3932, doi:10.5194/acp-15-3909-2015, 2015.

Mollner, A. K., Valluvadasan, S., Feng, L., Sprague, M. K., Okumura, M., Milligan, D. B., Bloss, W. J., Sander, S. P., Martien, P. T., Harley, R. A., McCoy, A. B., and Carter, W. P. L.: Rate of Gas Phase Association of Hydroxyl Radical and Nitrogen Dioxide, Science, 330, 646–649, doi:10.1126/science.1193030, 2010.

Müller, J.-F., Peeters, J., and Stavrakou, T.: Fast photolysis of carbonyl nitrates from isoprene, Atmos. Chem. Phys., 14, 2497–2508, doi:10.5194/acp-14-2497-2014, 2014.

Nguyen, T. B., Crounse, J. D., Teng, A. P., St. Clair, J. M., Paulot, F., Wolfe, G. M., and Wennberg, P. O.: Rapid deposition of oxidized biogenic compounds to a temperate forest, Proc. Natl. Acad. Sci. USA, 112, E392–E401, doi:10.1073/pnas.1418702112, 2015.

Orlando, J. J. and Tyndall, G. S.: Laboratory studies of organic peroxy radical chemistry: an overview with emphasis on recent issues of atmospheric significance, Chem. Soc. Rev., 41, 6294–6317, doi:10.1039/c2cs35166h, 2012.

Papale, D., Reichstein, M., Aubinet, M., Canfora, E., Bernhofer, C., Kutsch, W., Longdoz, B., Rambal, S., Valentini, R., Vesala, T., and Yakir, D.: Towards a standardized processing of Net Ecosystem Exchange measured with eddy covariance technique: algorithms and uncertainty estimation, Biogeosciences, 3, 571–583, 2006.

Paulot, F., Crounse, J. D., Kjaergaard, H. G., Kroll, J. H., Seinfeld, J. H., and Wennberg, P. O.: Isoprene photooxidation: new insights into the production of acids and organic nitrates, Atmos. Chem. Phys., 9, 1479–1501, doi:10.5194/acp-9-1479-2009, 2009.

Peeters, J., Müller, J.-F., Stavrakou, T., and Nguyen, V. S.: Hydroxyl Radical Recycling in Isoprene Oxidation Driven by Hydrogen Bonding and Hydrogen Tunneling: The Upgraded LIM1 Mechanism, J. Phys. Chem. A, 118, 8625–8643, doi:10.1021/jp5033146, 2014.

Perring, A. E., Bertram, T. H., Wooldridge, P. J., Fried, A., Heikes, B. G., Dibb, J., Crounse, J. D., Wennberg, P. O., Blake, N. J., Blake, D. R., Brune, W. H., Singh, H. B., and Cohen, R. C.: Airborne observations of total $RONO_2$: new constraints on the yield and lifetime of isoprene nitrates, Atmos. Chem. Phys., 9, 1451–1463, doi:10.5194/acp-9-1451-2009, 2009.

Perring, A. E., Bertram, T. H., Farmer, D. K., Wooldridge, P. J., Dibb, J., Blake, N. J., Blake, D. R., Singh, H. B., Fuelberg, H., Diskin, G., Sachse, G., and Cohen, R. C.: The production and persistence of $\Sigma RONO_2$ in the Mexico City plume, Atmos. Chem. Phys., 10, 7215–7229, doi:10.5194/acp-10-7215-2010, 2010.

Perring, A. E., Pusede, S. E., and Cohen, R. C.: An Observational Perspective on the Atmospheric Impacts of Alkyl and Multifunctional Nitrates on Ozone and Secondary Organic Aerosol, Chem. Rev., 113, 5848–5870, doi:10.1021/cr300520x, 2013.

Pusede, S. E., Gentner, D. R., Wooldridge, P. J., Browne, E. C., Rollins, A. W., Min, K.-E., Russell, A. R., Thomas, J., Zhang, L., Brune, W. H., Henry, S. B., DiGangi, J. P., Keutsch, F. N., Harrold, S. A., Thornton, J. A., Beaver, M. R., St. Clair, J. M., Wennberg, P. O., Sanders, J., Ren, X., VandenBoer, T. C., Markovic, M. Z., Guha, A., Weber, R., Goldstein, A. H., and Cohen, R. C.: On the temperature dependence of organic reactivity, nitrogen oxides, ozone production, and the impact of emission controls in San Joaquin Valley, California, Atmos. Chem. Phys., 14, 3373–3395, doi:10.5194/acp-14-3373-2014, 2014.

Pye, H. O. T., Luecken, D. J., Xu, L., Boyd, C. M., Ng, N. L., Baker, K. R., Ayres, B. R., Bash, J. O., Baumann, K., Carter, W. P. L., Edgerton, E. S., Fry, J. L., Hutzell, W. T., Schwede, D., and Shepson, P. B.: Modeling the Current and Future Roles of Particulate Organic Nitrates in the Southeastern United States, Environ. Sci. Technol., doi:10.1021/acs.est.5b03738, 2015.

Reuter, M., Buchwitz, M., Hilboll, A., Richter, A., Schneising, O., Hilker, M., Heymann, J., Bovensmann, H., and Burrows, J. P.: Decreasing emissions of NO_x relative to CO_2 in East Asia inferred from satellite observations, Nat. Geosci., 7, 792–795, doi:10.1038/ngeo2257, 2014.

Rindelaub, J. D., McAvey, K. M., and Shepson, P. B.: The photochemical production of organic nitrates from α-pinene and loss via acid-dependent particle phase hydrolysis, Atmos. Environ., 100, 193–201, doi:10.1016/j.atmosenv.2014.11.010, 2015.

Rivera-Rios, J. C., Nguyen, T. B., Crounse, J. D., Jud, W., St. Clair, J. M., Mikoviny, T., Gilman, J. B., Lerner, B. M., Kaiser, J. B., de Gouw, J., Wisthaler, A., Hansel, A., Wennberg, P. O., Seinfeld, J. H., and Keutsch, F. N.: Conversion of hydroperoxides to carbonyls in field and laboratory instrumentation: Observational bias in diagnosing pristine versus anthropogenically controlled atmospheric chemistry, Geophys. Res. Lett., 41, 8645–8651, doi:10.1002/2014GL061919, 2014.

Rohrer, F., Lu, K., Hofzumahaus, A., Bohn, B., Brauers, T., Chang, C.-C., Fuchs, H., Häseler, R., Holland, F., Hu, M., Kita, K., Kondo, Y., Li, X., Lou, S., Oebel, A., Shao, M., Zeng, L., Zhu, T., Zhang, Y., and Wahner, A.: Maximum efficiency in the hydroxyl-radical-based self-cleansing of the troposphere, Nat. Geosci., 7, 559–563, doi:10.1038/ngeo2199, 2014.

Rollins, A. W., Smith, J. D., Wilson, K. R., and Cohen, R. C.: Real Time In Situ Detection of Organic Nitrates in Atmospheric Aerosols, Environ. Sci. Technol., 44, 5540–5545, doi:10.1021/es100926x, 2010.

Russell, A. R., Valin, L. C., and Cohen, R. C.: Trends in OMI NO_2 observations over the United States: effects of emission control technology and the economic recession, Atmos. Chem. Phys., 12, 12 197–12 209, doi:10.5194/acp-12-12197-2012, 2012.

Russo, R. S., Zhou, Y., Haase, K. B., Wingenter, O. W., Frinak, E. K., Mao, H., Talbot, R. W., and Sive, B. C.: Temporal variability, sources, and sinks of C_1-C_5 alkyl nitrates in coastal New England, Atmos. Chem. Phys., 10, 1865–1883, doi:10.5194/acp-10-1865-2010, 2010.

Ryerson, T. B., Buhr, M. P., Frost, G. J., Goldan, P. D., Holloway, J. S., Hübler, G., Jobson, B. T., Kuster, W. C., McKeen, S. A., Parrish, D. D., Roberts, J. M., Sueper, D. T., Trainer, M., Williams, J., and Fehsenfeld, F. C.: Emissions lifetimes and ozone formation in power plant plumes, J. Geophys. Res., 103, 22 569–22 583, doi:10.1029/98JD01620, 1998.

Ryerson, T. B., Trainer, M., Angevine, W. M., Brock, C. A., Dissly, R. W., Fehsenfeld, F. C., Frost, G. J., Goldan, P. D., Holloway, J. S., Hübler, G., Jakoubek, R. O., Kuster, W. C., Neuman, J. A., Nicks Jr., D. K., Parrish, D. D., Roberts, J. M., Sueper, D. T., Atlas, E. L.,

Donnelly, S. G., Flocke, F., Fried, A., Potter, W. T., Schauffler, S., Stroud, V., Weinheimer, A. J., Wert, B. P., Wiedinmyer, C., Alvarez, R. J., Banta, R. M., Darby, L. S., and Senff, C. J.: Effect of petrochemical industrial emissions of reactive alkenes and NO_x on tropospheric ozone formation in Houston, Texas, J. Geophys. Res., 108, 4249, doi:10.1029/2002JD003070, 2003.

Saunders, S. M., Jenkin, M. E., Derwent, R. G., and Pilling, M. J.: Protocol for the development of the Master Chemical Mechanism, MCM v3 (Part A): tropospheric degradation of non-aromatic volatile organic compounds, Atmos. Chem. Phys., 3, 161–180, doi:10.5194/acp-3-161-2003, 2003.

Schneider, M., Luxenhofer, O., Deissler, A., and Ballschmiter, K.: C_1–C_{15} Alkyl Nitrates, Benzyl Nitrate, and Bifunctional Nitrates: Measurements in California and South Atlantic Air and Global Comparison Using C_2Cl_4 and $CHBr_3$ as Marker Molecules, Environ. Sci. Technol., 32, 3055–3062, doi:10.1021/es980132g, 1998.

Teng, A. P., Crounse, J. D., Lee, L., St. Clair, J. M., Cohen, R. C., and Wennberg, P. O.: Hydroxy nitrate production in the OH-initiated oxidation of alkenes, Atmos. Chem. Phys., 15, 4297–4316, doi:10.5194/acp-15-4297-2015, 2015.

Thornton, J. A., Wooldridge, P. J., and Cohen, R. C.: Atmospheric NO_2: In Situ Laser-Induced Fluorescence Detection at Parts per Trillion Mixing Ratios, Anal. Chem., 72, 528–539, doi:10.1021/ac9908905, 2000.

Valin, L. C., Russell, A. R., and Cohen, R. C.: Variations of OH radical in an urban plume inferred from NO_2 column measurements, Geophys. Res. Lett., 40, 1856–1860, doi:10.1002/grl.50267, 2013.

Washenfelder, R. A., Wagner, N. L., Dube, W. P., and Brown, S. S.: Measurement of Atmospheric Ozone by Cavity Ring-down Spectroscopy, Environ. Sci. Technol., 45, 2938–2944, doi:10.1021/es103340u, 2011.

Wolfe, G. M., Thornton, J. A., Yatavelli, R. L. N., McKay, M., Goldstein, A. H., LaFranchi, B., Min, K.-E., and Cohen, R. C.: Eddy covariance fluxes of acyl peroxy nitrates (PAN, PPN and MPAN) above a Ponderosa pine forest, Atmos. Chem. Phys., 9, 615–634, doi:10.5194/acp-9-615-2009, 2009.

Xiong, F., McAvey, K. M., Pratt, K. A., Groff, C. J., Hostetler, M. A., Lipton, M. A., Starn, T. K., Seeley, J. V., Bertman, S. B., Teng, A. P., Crounse, J. D., Nguyen, T. B., Wennberg, P. O., Misztal, P. K., Goldstein, A. H., Guenther, A. B., Koss, A. R., Olson, K. F., de Gouw, J. A., Baumann, K., Edgerton, E. S., Feiner, P. A., Zhang, L., Miller, D. O., Brune, W. H., and Shepson, P. B.: Observation of isoprene hydroxynitrates in the southeastern United States and implications for the fate of NO_x, Atmos. Chem. Phys., 15, 11 257–11 272, doi:10.5194/acp-15-11257-2015, 2015.

Xiong, F., Borca, C. H., Slipchenko, L. V., and Shepson, P. B.: Photochemical degradation of isoprene-derived 4,1-nitrooxy enal, Atmos. Chem. Phys., 16, 5595–5610, doi:10.5194/acp-16-5595-2016, 2016.

Zalakeviciute, R., Alexander, M. L., Allwine, E., Jimenez, J. L., Jobson, B. T., Molina, L. T., Nemitz, E., Pressley, S., VanReken, T. M., Ulbrich, I. M., Velasco, E., and Lamb, B. K.: Chemically-resolved aerosol eddy covariance flux measurements in urban Mexico City during MILAGRO 2006, Atmos. Chem. Phys., 12, 7809–7823, doi:10.5194/acp-12-7809-2012, 2012.
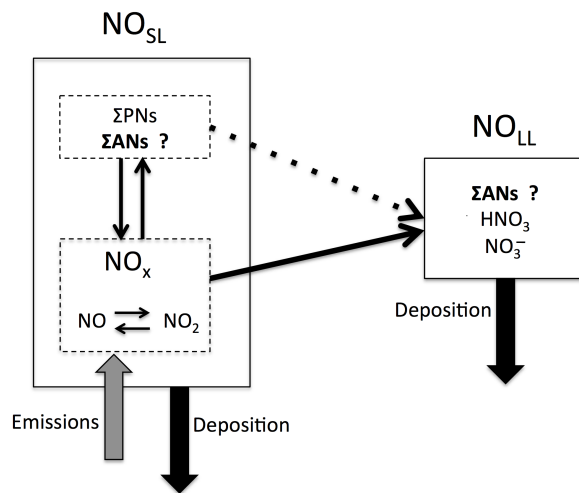
Figure 1. A schematic representation of the chemistry of NO_{SL} and NO_{LL}, showing the typical components of both classes.
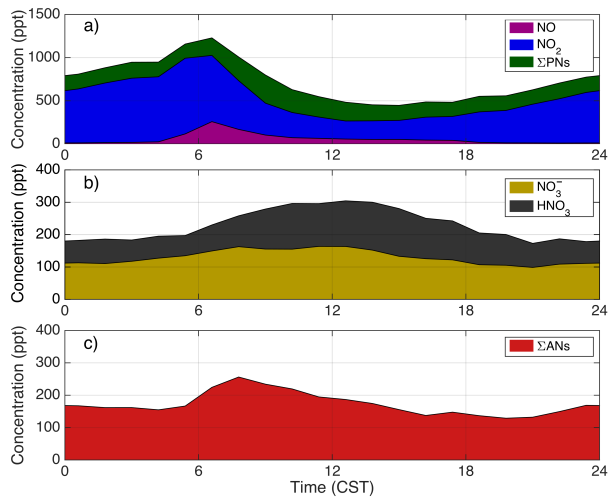
Figure 2. Diurnal cycle of measured reactive nitrogen species during SOAS. Reactive nitrogen species are classified as likely components of NO_{SL} (Fig. 2a), likely components of NO_{LL} (Fig. 2b) or unknown (Fig. 2c). The classification into NO_{SL} and NO_{LL} is based on typical summertime afternoon lifetimes. The measurement of HNO_3 represent nitric acid in the gas phase, while the measurement of NO_3^- represents inorganic nitrate in the particle phase. The measurement of ΣANs includes alkyl and multifunctional nitrates in both the gas and particle phase.
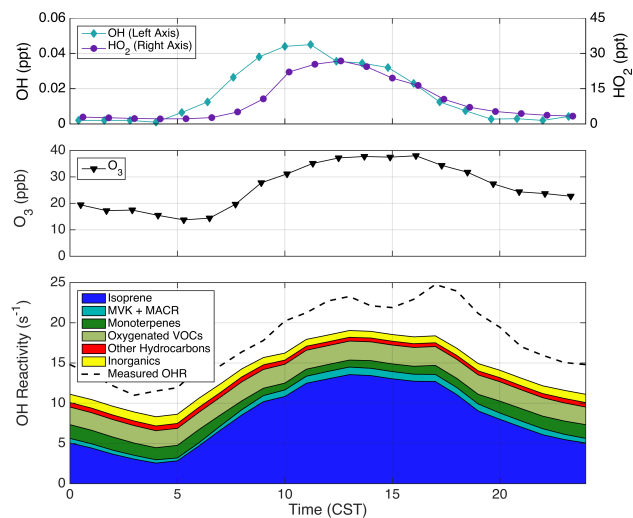
Figure 3. Diurnal cycle of OH, HO$_2$, O$_3$ and VOCs during SOAS. The top plot shows the concentration of OH and HO$_2$; the middle plot shows the concentration of O$_3$; the bottom plot shows the VOC Reactivity.
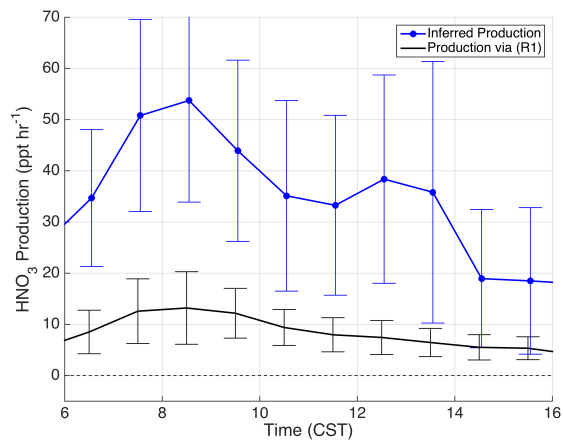
Figure 4. Production rates of nitric acid during SOAS calculated from the reaction of OH + NO$_2$ (black) and inferred from the concentration and deposition rate of nitric acid (blue). The vertical bars show the systematic and random uncertainty in the calculated rates, as described in the text.
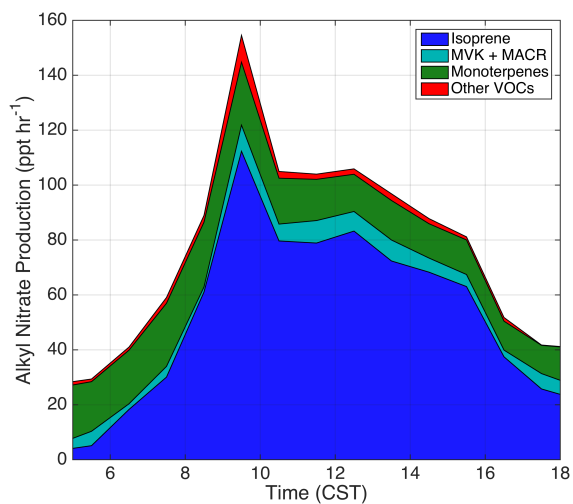
Figure 5. Average daytime production of ΣANs, categorized based on VOC precursors.
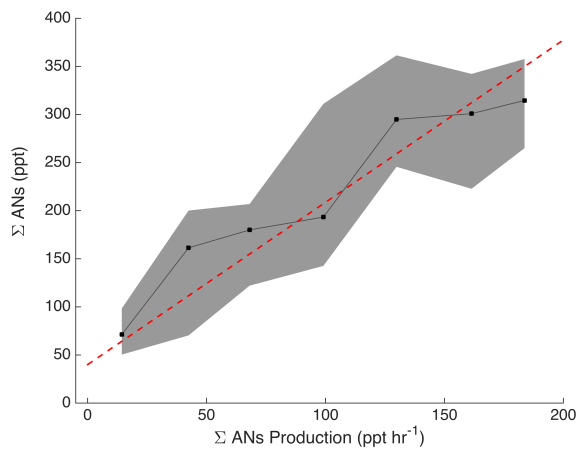
Figure 6. The concentration of ΣANs versus their production rate during the afternoon (12 pm – 4 pm). The black squares show the median in each bin, and the shaded grey area the interquartile range. A linear fit gives a slope of 1.7 hr.
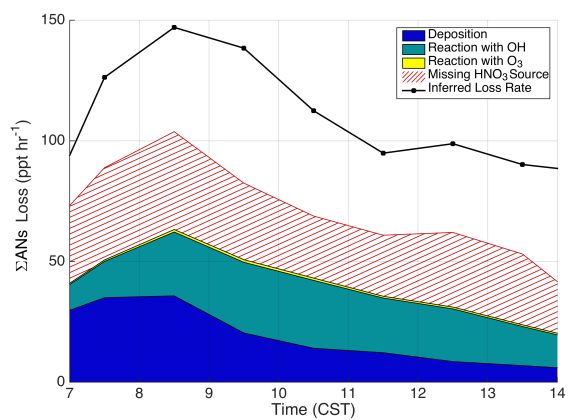
Figure 7. Loss rates and fates of ΣANs during SOAS. The black line shows the loss rate of ΣANs based on the difference between the calculated production rate and the observed change in concentration. The shaded areas show the rates of known ΣANs loss processes, and the hatched area shows the missing nitric acid source.
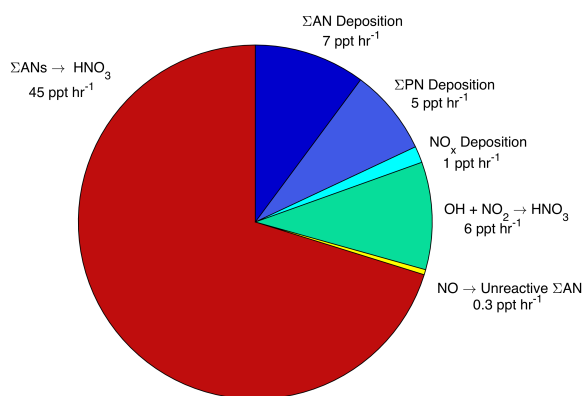
Figure 8. The average breakdown of NO_{SL} loss between 10 am and 2 pm during SOAS.